Free Volume and Interstitial Mesopores in Silica Filled Poly(1-trimethylsilyl-1-propyne) Nanocomposites

Petra Winberg,[†] Kristien DeSitter,[‡,§] Chris Dotremont,[‡] Steven Mullens,[‡] Ivo F. J. Vankelecom,[§] and Frans H. J. Maurer*,[†]

Department of Polymer Science & Engineering, Lund Institute of Technology, Lund University, P.O. Box 124, SE-221 00 Lund, Sweden; Flemish Institute for Technological Research (Vito), Boeretang 200, B-2400 Mol, Belgium; and Centre for Surface Chemistry and Catalysis, Faculty of Applied Bioscience and Engineering, Katholieke Universiteit Leuven, Kasteelpark Arenberg 23, B-3001 Leuven, Belgium

Received December 21, 2004; Revised Manuscript Received February 8, 2005

ABSTRACT: The free volume sizes and interstitial mesopore sizes in poly(1-trimethylsilyl-1-propyne) (PTMSP)/silica nanocomposites and the correlation between nitrogen permeability and cavity sizes were studied with positron annihilation lifetime spectroscopy (PALS) at filler concentrations between 0 and 50 wt %. A bimodal free volume distribution was observed for PTMSP, and the size of the larger free volume cavities was significantly increased upon addition of hydrophobic fumed silica. Nanometer-sized interstitial cavities in filler agglomerates were observed in all PTMSP/fumed silica nanocomposites and in neat hydrophobic fumed silica. The radius of these interstitial mesopores in the nanocomposites decreased with decreasing filler concentration. A strong correlation between nitrogen permeability and the volume of the interstitial mesopores in the nanocomposite membranes was observed.

Introduction

The use of polymeric materials in gas and vapor separation membranes has received much attention in the past decades.[1,2] Much work has been focused on gaining insight into the relations between the structure of polymers and the performance of polymeric membranes in terms of permeability and selectivity.[1−9] Understanding the relations between polymer structure and permeability and selectivity of a polymer membrane enables tailoring of the structure of polymer materials for specific gas and vapor separation purposes. The permeation of gases and vapors through a polymer is generally described as a solution−diffusion process, and the permeability of a penetrant molecule through a polymer is the product of its solubility and diffusivity.[3] The gas diffusivity is dependent on the free volume sizes in the polymer, the size of the penetrant molecule, and the segmental mobility of the polymer.[9−12] Generally, larger free volume sizes, smaller penetrants, and higher mobility result in higher diffusion rates. Close to or below the glass transition temperature, the polymer exhibits low segmental mobility and is in a nonequilibrium state, and the solution and diffusion mechanisms become more complex as compared to the rubbery state. Solution of gases in glassy polymers is described by two separate solution mechanisms, dissolution, present also in rubbery polymers, and sorption in preexisting micropores, which only exist in glassy polymers.[13−15] Because of the low segmental mobility, the diffusivity is time-dependent and the rearrangement of polymer chains, to accommodate a penetrant molecule, does not occur instantaneously.[3] The mobility and free volume sizes in polymers and consequently also the diffusivity can further be influenced by frozen-in internal stresses in glassy polymers.[3,16,17] The ideal selectivity of polymers for certain penetrant pairs is the ratio between their respective permeabilities. The selectivity of polymers can be based on a size-selective mechanism meaning smaller penetrant molecules diffuse faster than larger penetrants due to a higher fraction of free volume cavities of sufficient size being available for smaller penetrants. Alternatively, the selectivity can originate from differences in solubility between different penetrants, caused by either differences in vapor pressure or ability to realize specific interaction with the polymer.[18] Size selectivity is usually encountered in the case of glassy polymer membranes, which have smaller free volume sizes and are characterized by high selectivities and low permeation rates. Solubility−selectivity generally occurs in rubbery polymer membranes, which have larger free volume sizes and higher segmental mobility. Rubbery polymers typically show lower selectivity and higher permeation. One of the exceptions to the generally observed transport mechanisms in glassy and rubbery polymers is poly(1-trimethylsilyl-1-propyne) (PTMSP). PTMSP has exceptionally large free volume cavity sizes and low mobility (glass transition temperature > 280 °C) due to the presence of double bonds in the backbone and bulky trimethylsilyl side groups creating a rigid structure with low intersegmental packing.[19] PTMSP, in contrast to other glassy polymers, has a low selectivity, mainly based on solubility selectivity and high permeation rates.[20−22]

Tailoring polymeric materials for gas and/or vapor separation membranes can be achieved by creating an accurate free volume size distribution in the polymer.[9,10,12] The free volume size distributions can be modified for example by incorporating side groups in the backbone, which act as spacers or by substituting units in the backbone with units of a different flexibility.[1,2,7,9,23,24] Recent research has shown that the presence of inorganic fillers can be another means of influencing the free volume sizes and mobility of a

[†] Lund University.
[‡] Flemish Institute for Technological Research (Vito).
[§] Katholieke Universiteit Leuven.
* Corresponding author: e-mail Frans.Maurer@polymer.lth.se; Fax +46 46 222 4115; phone +46 46 222 9149.

10.1021/ma047369j CCC: $30.25
Published on Web 03/30/2005

polymer. Using techniques such as nuclear magnetic resonance,[25−27] dielectric spectroscopy,[28,29] differential scanning calorimetry,[30−32] and positron annihilation lifetime spectroscopy,[33−37] it has been observed that the interactions between polymer segments and surfaces induce altered chain dynamics, glass transition temperature, and free volume sizes as compared to the bulk state.

Recently, a possibility to tailor the free volume sizes of glassy polymers for gas membrane applications by introducing high-surface-area silica particles in a polymer matrix[38−41] has been reported. Merkel et al. observed that the addition of silica particles to high-free-volume polymers, such as poly(4-methyl-2-pentyne) (PMP) and PTMSP, increased the permeability and the free volume sizes in the polymer. The increased permeability upon addition of silica is unexpected since the presence of impenetrable phases, such as nonporous fillers or crystallites in an amorphous matrix, usually decrease the permeability of gases since diffusants have to travel a tortuous path, which increases the average diffusion length.[42] The increased permeability was ascribed to increased free volume sizes in the polymer, which was caused by the high-surface-area silica particles disrupting the packing of the polymer chains. Merkel et al. also observed an increase of both selectivity and permeability when silica was added to PMP, which is remarkable with respect to the generally observed inverse relationship between permeability and selectivity.[38,39]

Important aspects when introducing high-surface-area fillers into a polymer matrix are the dispersion of the filler particles and the closely linked interfacial interaction between filler and polymer matrix.[3,43−45] Weak interfacial interaction can lead to the formation or preservation of filler aggregates and/or the creation of voids at the interface. Aggregates of nanosized fillers, which are normally in the micron length scale, can also enclose interstitial volume inaccessible to polymer segments and reduce the effective surface area of the filler and the possibility of surface-induced tailoring of the free volume sizes. These enclosed voids at the filler surface can also act as adsorption sites and/or offer a faster route of transportation, through convection rather than diffusion, which is likely to lead to altered selectivity and permeability.[3,44,45]

In light of recent research showing a promising but not fully understood increase in permeability, and in some cases also increased selectivity, in glassy high-free-volume polymers upon incorporating nonporous nanosized fillers into the polymer matrix, it is of importance to gain deeper insight into the changes in free volume structure of these polymers. In this paper the effect of nanosized nonporous hydrophobic fumed silica in a PTMSP matrix on the polymer free volume sizes and the nanometer-sized interstitial cavities in the filler agglomerates is studied with positron annihilation lifetime spectroscopy (PALS). In addition, the correlation between gas permeability and the size of free volume and interstitial mesopores is reported. PALS is a technique that probes the free volume cavities by measuring the lifetime of orthopositronium (o-Ps) before annihilation in the free volume regions of the polymer. The lifetime of o-Ps (normally 2−5 ns) is a direct measure of the free volume cavity size. It is also possible to detect annihilation of o-Ps in the interstitial cavities of fumed silica, which are mesopores and roughly 10 times the size of the free volume cavities, by extending the time window of the lifetime spectrum. The free volume cavity sizes in PTMSP and the interstitial cavity sizes in filler agglomerates were studied as a function of filler content ranging from 0 to 50 wt % fumed silica.

Materials and Methods

The PTMSP (SSP-070) used in this study was obtained from Gelest Inc. Fumed SiO_2 (Cabosil TS-530) with a surface area of 225 m^2/g and a density of 2.2 g/cm^3 treated with hexamethyldisilazane was obtained from Cabot Corp., Germany. On the basis of the surface area and density of the fumed silica and assuming a spherical shape, the particle diameter can be estimated to about 12 nm. The PTMSP and PTMSP/silica membranes were prepared by a three-step solvent casting procedure. Silica particles were initially dissolved in toluene (Merck, >99%) at room temperature with ultrasonic treatment for 30 min followed by stirring with a magnetic stirrer for 3 h. The PTMSP was then dissolved in the silica/toluene dispersion with magnetic stirring for 4 days, after which the solution was cast on a glass plate. The total concentration of PTMSP and silica in the dispersion was 5 wt %. The toluene was then allowed to evaporate at ambient conditions for 4 days followed by drying in a vacuum at 80 °C for 2 h. The cast membranes were about 100 μm thick. The Cabosil contents in the membranes were 0, 10, 20, 30, and 50 wt % and are referred to as PTMSP, PTMSP10, and so on in the following text. Flat sheet disks used in permeability and positron annihilation lifetime spectroscopy (PALS) measurement were cut from the same membrane. For PALS measurements 12 stacked disks were used on either side of the positron source. The samples were stored in plastic bags at ambient conditions for a period of about 4 weeks before the measurements.

Positron Annihilation Lifetime Spectroscopy (PALS). Positron annihilation lifetime spectroscopy employs a radioactive material which emits positrons during its decay. The positron source (^{22}Na) was encapsulated between sheets of Kapton on both sides. The encapsulated radioactive material is sandwiched between two pieces of the material, which is under study. In the case of unfilled PTMSP and PTMSP/fumed silica nanocomposites, the pieces were 12 membranes in the shape of disks stacked on either side of the positron source. In the case of neat fumed silica, manually compacted powder yielding an approximately 15 mm thick layer was placed on both sides of the encapsulated source and fixed in place by a second set of Kapton sheets. When the source emits a positron, a 1.28 MeV γ-ray is simultaneously emitted. The positron enters the polymer and annihilates with an electron, emitting two γ-rays of 0.51 MeV. There are at least three different ways for positrons to annihilate in a polymer material. Free positrons can annihilate directly with electrons in 0.3−0.5 ns. The positron can also form a metastable bound state called positronium, with an electron originating from the surrounding polymer. Positronium can be formed in two states. Parapositronium (p-Ps) is formed by two particles with opposite spin, and orthopositronium (o-Ps) is formed if the spins of the particles are parallel. In a vacuum p-Ps and o-Ps annihilate intrinsically with mean lifetimes of 0.125 and 142 ns, respectively. In polymers, o-Ps can pick off an electron of opposite spin from the surrounding medium, and the lifetime is shortened to 1−5 ns depending on the average electron density surrounding the o-Ps. The lifetimes of p-Ps, free positrons, and o-Ps are referred to as τ_1, τ_2, and τ_3. It has been shown that o-Ps is formed and annihilates in regions of low electron density.[46] In a polymer, the low electron density regions are the free volume sites of the polymer, and the lifetime of o-Ps is therefore related to the size of the free volume cavities. Assuming that the positronium is localized in a spherical potential well having an infinite potential barrier of radius R_0 with an electron layer thickness ΔR equal to 0.166 nm,[47,48] the radius $R = R_0 - \Delta R$ of the free volume cavity can be estimated by eq 1a[47,49] and the volume of the equivalent sphere by eq 1b, where τ_3 is in nanoseconds.

$$\tau_3 = 0.5\left(1 - \frac{R}{R_0} + \frac{1}{2\pi}\sin\frac{2\pi R}{R_0}\right)^{-1} \quad (1a)$$

$$V(\tau_3) = \frac{4\pi R^3}{3} \quad (1b)$$

The time difference between the start γ-ray emitted at the birth of the positron and the stop γ-ray emitted at the annihilation was recorded by employing a fast−fast coincidence system. The source was placed between two identical samples during the measurements. The count rate was 90 per second, and at least 2 million counts were collected in each spectrum; the measurements were performed at ambient conditions. The spectra were evaluated using POSITRONFIT[50] and the algorithm Maximum Entropy for Lifetime Analysis (MELT).[51] POSITRONFIT is a data processing system based on a model function consisting of a sum of decaying exponentials convoluted with the resolution function of the lifetime spectrometer, plus a constant background. The system fits a fixed number of lifetimes to the spectra, and the results are given as mean lifetimes and respective intensities. The best fit of the experimental data of positron annihilation in SiO_2 and PTMSP using POSITRONFIT was achieved by using a four-component analysis. In the case of PTMSP/SiO_2 membranes a five-component fit yielded the best fit to the experimental data. MELT resolves the lifetime data in a lifetime distribution consisting of a number of peaks and the average lifetimes, and the corresponding intensities are calculated as the mass center and relative area under the peaks. The number of peaks is not fixed. The entropy weight was varied between 10^{-4} and 10^{-7}, and the maximum probability was chosen. The cutoff value was 10^{-3}. The time resolution used in both evaluation programs was determined to be 0.32 ns.

Results and Discussion

Free Volume and Interstitial Cavity Size in PTMSP/SiO_2 Membranes. Table 1 shows the lifetimes and intensities of the different positron annihilation processes in hydrophobic SiO_2 and unfilled PTMSP membranes. Positrons entering SiO_2 are most likely to annihilate as parapositronium (p-Ps) and free positrons as evidenced by the high intensity of the two shorter lifetimes τ_1 and τ_2. A small fraction of the positrons annihilate through pick-off annihilation of orthopositronium (o-Ps), resulting in two longer lifetimes (τ_3 and τ_5), which are 3.2 and 52 ns with respective intensities of 4.2 and 4.7%.

τ_3 and τ_5 correspond to cavities with a mean radius of 0.38 and 1.27 nm, respectively (eq 1). The shorter o-Ps lifetime (τ_3) has been reported to originate from o-Ps annihilation within in the particles[52] and is therefore a measure of free volume cavity size in the amorphous SiO_2 particles. The longer o-Ps lifetime (τ_5), which corresponds to cavity sizes much larger than any polymer free volume cavities, has been reported to be a consequence of o-Ps annihilating in the interstitial cavities of the filler agglomerates.[52] Fumed silica, which consists of aggregates of nonporous nanometer-sized SiO_2 particles linked together in weak networks, can macroscopically be considered a porous medium.[53] The size of the nonporous particles and the coordination number, meaning the number of particle contacts per particle, control the average pore diameter in the fumed silica.[53] The pore size generally decreases with decreasing particle size and increasing coordination number. Particle packing arrangement with high regularity is unlikely in actual fumed silica powders and gels. It is however interesting to compare the interstitial cavity size in the filler agglomerates calculated from τ_5 (eq 1), which was found to be 1.27 nm in radius, to the pore sizes in idealized regular packing structures of fumed silica particles. A lower coordination number of 4, corresponding to tetragonal packing of particles with a radius R, yields a radius of a spherical pore inscribed in the cavities equal to $1.0R$.[53] A higher coordination number of 12, corresponding to hexagonal close packing of particles, yields a radius of a spherical pore inscribed in the cavities equal to $0.225R$.[53] Without excluding the presence of larger interstitial cavities in the fumed silica, a very simplified estimation, based on the fumed silica particle diameter (12 nm), suggests that the interstitial cavity size in the fumed silica calculated from τ_5 (eq 1) corresponds to filler agglomerates with a higher coordination number. It appears that although the mean interstitial cavity size (eq 1) is calculated from relatively long lifetimes and does not take into account the irregular shape of the interstitial cavities,[54,55] the lifetime still represents the size of interstitial pores in fumed silica. Considering the presence of these large interparticle voids in hydrophobic fumed silica and the potential use of hydrophobic fumed silica and other SiO_2 powders in polymer nancomposite membranes for gas/vapor separation purposes, it should be noted that these large cavities, if present also when SiO_2 particles are embedded in a PTMSP matrix, will most likely have a strong influence on the permeability and selectivity of both gases and vapors in the corresponding membrane. The cavities can act as absorption sites and/or offer a faster route of transportation for penetrants, which is likely to lead to changes in size selectivity and permeation rates.

Table 1. Lifetimes and Intensities of Positron Annihilation in PTMSP and Fumed Silica

	τ_1 (ns)	τ_2 (ns)	τ_3 (ns)	τ_4 (ns)	τ_5 (ns)
PTMSP	0.1 ± 0.01	0.4 ± 0.01	2.1 ± 0.20	6.3 ± 0.08	
SiO_2	0.3 ± 0.01	0.8 ± 0.02	3.2 ± 0.02		52.7 ± 0.9
	I_1 (%)	I_2 (%)	I_3 (%)	I_4 (%)	I_5 (%)
PTMSP	13.1 ± 0.9	43.2 ± 0.7	10.1 ± 0.6	33.7 ± 0.9	
SiO_2	76.9 ± 0.6	14.1 ± 0.6	4.2 ± 0.1		4.7 ± 0.1

The contribution of o-Ps pick-off annihilation in PTMSP is relatively high, resulting in two mean lifetimes of 2.1 ns (τ_3) and 6.3 ns (τ_4) with intensities of 10 and 34%, respectively. The mean lifetimes and intensities as well as the bimodal shape of the o-Ps annihilation lifetime distribution, which is uncommon in most polymers, are in good agreement with previous studies.[56,57] The two o-Ps lifetimes describe the annihilation of o-Ps in smaller free volume cavities (τ_3) and larger, possibly interconnected, free volume cavities (τ_4).[21,22,57] The corresponding radius of free volume cavities obtained from τ_3 and τ_4 (eq 1) are 0.3 and 0.53 nm, which is in good agreement with molecular modeling studies.[58] The free volume radius in glassy polymers are generally in the range of 0.2 and 0.3 nm, which is much smaller than the size of the larger free volume cavities in PTMSP. The large free volume sizes in PTMSP agree well with the fact that PTMSP has the highest permeability among all polymers.

Considering the observed presence of large cavities with a radius of about 1.27 nm in hydrophobic SiO_2 particle agglomerates, it is, from a membrane application point of view, of great interest to investigate whether these mesopores are still present when SiO_2 particles are embedded in a PTMSP matrix. Figure 1 displays the interstitial cavity radius in filler agglomerates in PTMSP/SiO_2 nanocomposites as a function of

Table 2. Lifetimes and Intensities of Positron Annihilation in PTMSP/Hydrophobic Fumed Silica Nanocomposites

	τ_1 (ns)	τ_2 (ns)	τ_3 (ns)	τ_4 (ns)	τ_5 (ns)
PTMSP10	0.10 ± 0.01	0.35 ± 0.01	2.1 ± 0.1	6.5 ± 0.1	29 ± 3
PTMSP20	0.11 ± 0.01	0.37 ± 0.01	2.1 ± 0.2	6.8 ± 0.2	31 ± 3
PTMSP30	0.11 ± 0.01	0.38 ± 0.01	2.2 ± 0.1	7.5 ± 0.2	34 ± 2
PTMSP50	0.12 ± 0.01	0.39 ± 0.01	1.9 ± 0.1	7.7 ± 0.2	40 ± 1
	I_1 (%)	I_2 (%)	I_3 (%)	I_4 (%)	I_5 (%)
PTMSP10	13.0 ± 0.6	44.2 ± 0.4	9.7 ± 0.5	31.6 ± 0.6	1.5 ± 0.2
PTMSP20	14.2 ± 0.7	43.9 ± 0.2	9.2 ± 0.5	29.5 ± 0.6	2.5 ± 1.0
PTMSP30	14.6 ± 0.6	44.9 ± 0.7	10.9 ± 0.3	24.1 ± 0.2	5.6 ± 0.3
PTMSP50	15.3 ± 0.9	47.1 ± 0.7	8.4 ± 0.1	16.9 ± 0.1	12.4 ± 0.1

filler content. The corresponding lifetimes are shown in Table 2.

The mean radius of the measured interstitial cavities increases with increasing filler content from 1.0 nm in the PTMSP10 membrane to 1.27 nm in fumed silica. The increase of the mesopore radius with increasing filler content shows that the mesopore radius of the SiO_2 particles is dependent on the fraction of particles in the polymer matrix. When fumed silica is dispersed in a solvent, and the solvent is subsequently removed, the weakly linked network of fumed silica agglomerates/particles will collapse due to surface tension forces and the particle packing and coordination number will be increased.[53] Adding polymer to the filler dispersion will result in polymer segments being present between the randomly distributed SiO_2 particles and agglomerates, which thereby can reduce the apparent size of the interstitial cavities. Such partial filling of interstitial cavities in the filler agglomerates can be expected to be more efficient at low filler concentration since more polymer segments will be available per filler surface area, which could explain the observed decrease of the cavity radius with decreasing filler content. Figure 1 also shows the interstitial cavity radius measured in SiO_2 particle network recovered from PTMSP50 membranes. The SiO_2 was recovered by dissolving and removing the polymer leaving the SiO_2 particle structure in the membrane relatively undisturbed. The cavity radius measured in these particles after removal of the polymer matrix was increased to about 1.27 nm, which is 0.12 nm larger than the original PTMSP50 membrane and essentially the same as in the neat hydrophobic SiO_2. This increase in interstitial volume in PTMSP/SiO_2 membrane when the polymer is removed supports the concept of polymer segments partly covering the interstitial cavities in the PTMSP/SiO_2 membranes and thereby reducing the apparent cavity size.

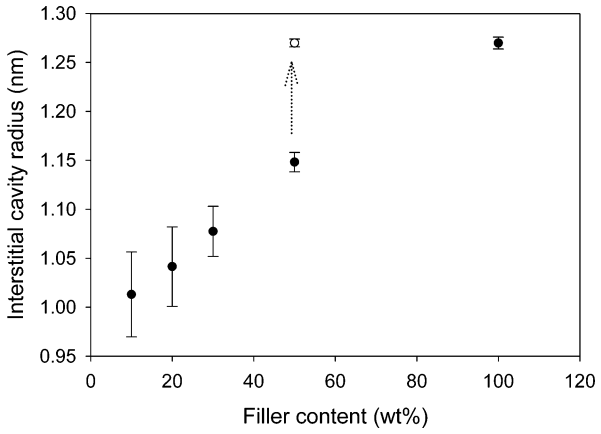

Figure 1. Interstitial cavity radius in PTMSP/hydrophobic fumed silica nanocomposite membranes (●) at room temperature, calculated from eq 1 and τ_5, as a function of silica content and interstitial cavity radius in silica recovered from PTMSP50 membranes (○). Arrow indicates the shift of the interstitial cavity radius upon removal of the polymer matrix in PTMSP50.

Figur 2 shows the radius of the large polymer free volume cavities in PTMSP/SiO_2 nanocomposites as a function of filler content. The free volume cavity size increases significantly and systematically from 0.53 nm in unfilled PTMSP to 0.58 nm in PTMSP50. This

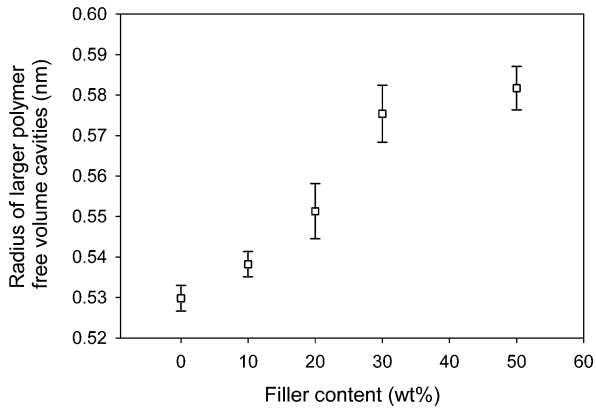

Figure 2. Large free volume cavity radius in PTMSP/hydrophobic fumed silica nanocomposite membranes at room temperature, calculated from eq 1 and τ_4, as a function of silica content.

increase in cavity size with filler content indicates that the filler surface induces changes in the polymer free volume size, which will increase with increasing filler content. The relatively large increase in free volume cavity size even at the lower filler contents indicates that free volume changes in the polymer are induced even relatively far from the filler surface. Assuming complete coverage of the filler surface and a polymer density of about 0.8 g/cm^3,[22] it can be estimated that in the PTMSP20 membrane, for which a significant increase in the mean free volume cavity size was measured, about 80% of the polymer is separated by more than 5 nm from a filler surface. Incomplete coverage of the filler surface, which is more likely in a nanocomposite and especially considering the observed presence of interstitial cavities in the filler agglomerates, would result in an increase of the fraction of polymer which is separated by more than 5 nm from a filler surface. In most studies it has been observed that the length scale at which a surface will influence the mobility and the free volume sizes of a polymer is usually in the range of 1−5 nm.[26,28,34,59] However, the length scale of the surface effects can be expected to be influenced by the polymer mobility, and therefore it is possible that the relatively large effects of hydrophobic SiO_2 particles on the larger free volume cavity sizes in PTMSP reflects

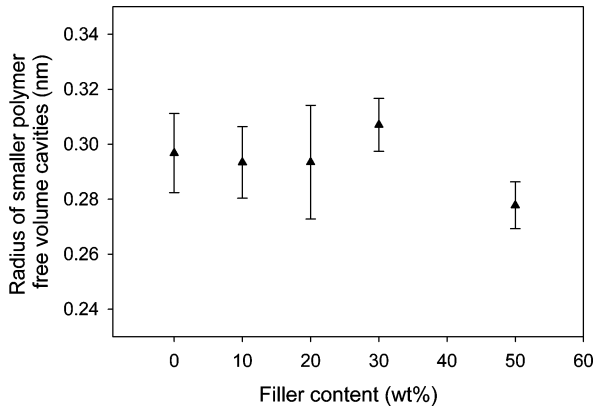

Figure 3. Small free volume cavity radius in PTMSP/hydrophobic fumed silica nanocomposite membranes at room temperature, calculated from eq 1 and τ_3, as a function of silica content.

the low mobility of the PTMSP backbone. It has previously been observed that unfilled PTMSP, in terms of free volume cavity sizes and permeability, is unusually sensitive to aging and casting procedures,[56,57] which suggests that the large free volume sizes and high permeability in unfilled PTMSP is to a large extent due to nonequilibrium properties promoted by the intrinsic low mobility of the polymer and the commonly used casting conditions. It is therefore possible that the observed increased free volume sizes in PTMSP/SiO_2 membranes are nonequilibrium effects. Increased free volume sizes in PTMSP upon addition of fumed silica has previously been observed by Merkel et al. and was then ascribed to disruption of the polymer chain packing by the presence of nanosized silica particles.[41] It should be noted that although there is a strong correlation between free volume sizes and permeability of gases and vapors in conventional polymer membranes, it can be expected that in the case of PTMSP/SiO_2 nanocomposite membranes the large interstitial cavities (1−1.3 nm in radius) will have a considerable effect on the permeability of these membranes.

Figure 3 shows the small free volume cavity sizes in PTMSP/SiO_2 composites as a function of filler content. The mean small free volume radius in PTMSP is about 0.29 nm and does not show any clear dependence on filler content, suggesting that the filler particles have a negligible effect on this part of the bimodal free volume size distribution of the polymer.

Figure 4 shows the intensities of the o-Ps annihilation in PTMSP/SiO_2 nanocomposites corresponding to o-Ps annihilation in the interstitial mesopores of the filler agglomerates (I_5), the larger polymer free volume cavities (I_4), and the smaller polymer free volume cavities (I_3). I_5 increases from about 2% in PTMSP10 to about 12% in PTMSP50, which is higher than I_5 in the neat hydrophobic SiO_2 powder. This behavior of I_5 is rather unexpected since it has been shown that a linear relationship (eq 2) exists between the weight fraction of the components and the total o-Ps, p-Ps, and free positron intensity for conventional polymer composites with micron-sized filler particles and polymer blends with micron-sized grains,[60,61] where c, p, and m indicate composite, particle, and matrix, respectively.

$$I_c = w_p I_p + (1 - w_p) I_m$$

I_5 in PTMSP/SiO_2 composites is higher than the linear weight addition (eq 2) prediction based on the experimental annihilation data in PTMSP and hydrophobic SiO_2. However, since it has been observed that τ_5 originates from o-Ps annihilation in interstitial cavities, the increase of I_5 in the composite, as compared to the predictions (eq 2), could be explained by shrinkage of the particle structure after immersion in a solvent during the casting procedure. Fumed SiO_2 in its powdery form has a very low density and larger interparticle cavities. When o-Ps resides in very large (r > 2 nm) cavities, it is likely to annihilate intrinsically after 142 ns, resulting in three γ-rays, which will not be effectively detected by this experimental setup. Closer packing of particles, although random, as occurs after dispersion in a solvent or polymer solution with subsequent drying,[53] can therefore increase the probability of pick-off annihilation of o-Ps in interparticle cavities and consequently increase I_5. The medium o-Ps intensity (I_4) decreases from 34% in unfilled PTMSP to 17% in PTMSP50. The relationship between I_4 and filler content, which approaches zero at 100 wt % SiO_2, shows, according to eq 2, that this lifetime component originates from o-Ps annihilation in the polymer phase. I_3 decreases from 10% in unfilled PTMSP to 8% in PTMSP50, which is roughly in agreement with a linear weight addition of I_3 in the respective components according to eq 2.

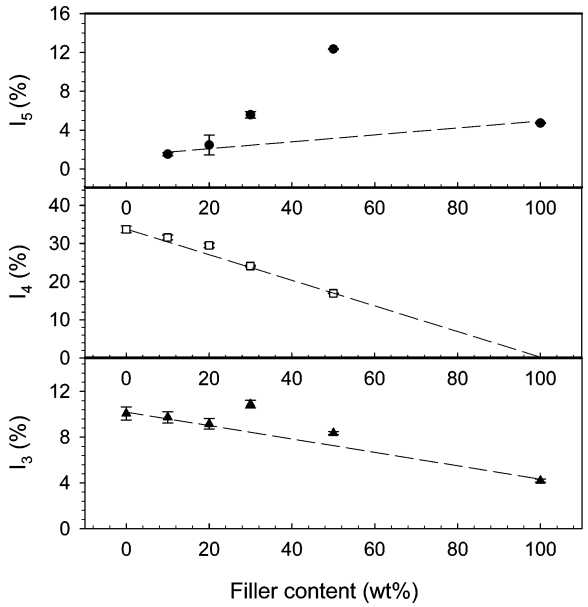

Figure 4. Intensities of o-Ps annihilation in PTMSP/hydrophobic fumed silica nanocomposites at room temperature. Lines represent the predictions according to linear weight addition (eq 2) based on the experimental annihilation data from PTMSP and hydrophobic fumed silica.

Cavity Size Distributions in PTMSP/SiO_2 Membranes. Considering that not only the mean interstitial cavity size in filler agglomerates and the mean free volume size in polymers but also the distribution of sizes will affect the diffusion rates in polymers, it is of interest to investigate the effect of incorporating hydrophobic SiO_2 into a PTMSP matrix on the free volume size distribution in PTMSP.

Figure 5 shows the cavity size distributions of PTMSP/SiO_2 composites as a function of filler content calculated with MELT. The lifetime distribution of τ_5, originating from o-Ps annihilation in the interstitial cavities in SiO_2 powder, is sharpened when the particles are incorporated into the PTMSP matrix at high load-

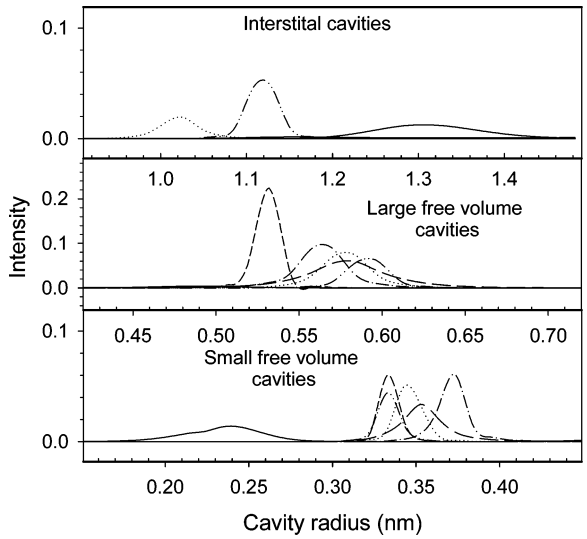

Figure 5. Distribution of the interstitial and free volume cavity radius in PTMSP/hydrophobic fumed silica nanocomposite membranes at room temperature calculated with the MELT program: (—) 100 wt % silica, (-•••-) 50 wt % silica; (•••) 30 wt % silica; (– – –) 20 wt % silica; (-•-•-) 10 wt % silica; (- - -) unfilled PTMSP.

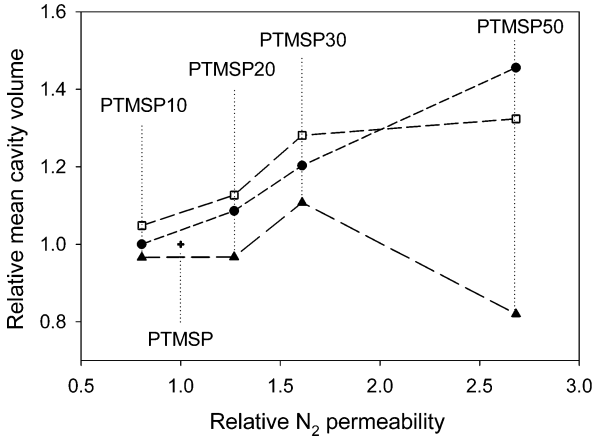

Figure 6. Relative nitrogen permeability ($P_{composite}$ (barrer)/$P_{unfilled\ polymer}$ (barrer)) in PTMSP/hydrophobic fumed silica nanocomposite membranes as a function of the relative mean cavity volume at room temperature: (●) relative interstitial cavity volume ($V_{interstitial-composite}$ (nm^3)/$V_{Interstitial-PTMSP10}$ (nm^3)); (□) relative large free volume cavity volume ($V_{large\ free\ volume-composite}$ (nm^3)/$V_{large\ free\ volume-unfilled\ polymer}$ (nm^3)); (▲) relative small free volume cavity volume ($V_{small\ free\ volume-composite}$ (nm^3)/$V_{small\ free\ volume-unfilled\ polymer}$ (nm^3)); (+) unfilled PTMSP membrane. The mean interstitial, large free volume, and small free volume cavity volumes (V) are calculated from the respective cavity radius (R) according to $V = 4\pi R^3/3$. Dashed lines are for guidance.

ing. At lower loading it was not possible to resolve the interstitial cavity size distribution due to its low intensity. The large polymer free volume cavity size distribution appears to be broader in the composites than in the unfilled polymer. This broadening agrees well with the observed increase of the mean free volume size since it is likely that while a fraction of the polymer in the PTMSP exhibits increased free volume sizes there will also be polymer segments relatively far from the filler surface exhibiting bulk free volume properties. The small polymer free volume cavity size distribution in PTMSP/SiO_2 does not show any clear dependence on the SiO_2 content. It should also be noted that average lifetimes and intensities, as well as the number of lifetime components, obtained with MELT agree well with the results from POSITRONFIT.

Permeability. The PALS measurements showed that large interstitial cavities are present in the filler agglomerates in PTMSP/SiO_2 nanocomposites. In addition, significant changes in the polymer free volume structure were observed. These findings encourage the exploration of a correlation between gas permeability and interstitial or free volume cavity sizes in PTMSP/SiO_2 nanocomposites.

Figure 6 shows the relative nitrogen permeability in PTMSP/SiO_2 nanocomposite membranes as a function of the relative volume of interstitial and free volume cavities in silica filled and unfilled membranes, respectively. The nitrogen permeability in the PTMSP/SiO_2 membranes is initially decreased upon addition of 10 wt % hydrophobic SiO_2 but increases thereafter with increasing filler content. This relationship between the permeability and filler content (>10 wt %), which contradicts the commonly observed reduction of permeability upon incorporating nonporous fillers into a polymer matrix, was observed also for other gases and vapors.[62] For PTMSP/SiO_2 membranes (>10 wt %) a clear correlation between the interstitial cavity volume and the nitrogen permeability is observed. The nitrogen permeability is almost tripled as the relative interstitial cavity volume increased with about 45%. A correlation between the large free volume cavity volume and the permeability can also be observed, while the small free volume cavity volume appears to have no apparent correlation to the nitrogen permeability. On the basis of these results, it is possible that the increased permeability is caused by the presence of interstitial cavities and not by increased free volume cavity volume. Interstitial cavities in the filler agglomerates can increase the permeability of gases in nanocomposites, as compared to a nanocomposite with complete coverage of the filler surface, by increasing the diffusivity of the gas[44,45] and/or by increasing the solubility of the gas.[42] Considering the rather significant increase in permeability and the size of the interstitial cavities, which is much larger than the size of the penetrant, it seems likely that both the diffusivity and the solubility of the membranes are affected. Previous studies have shown that increased diffusivity in filled rubbers, due to incomplete coverage of the filler surface, occurs at relatively high filler concentrations (>50 vol %).[42] However, it is known that due to low segmental mobility glassy polymeric membranes filled with nanosized particles are more prone to enclose defects, caused by preservation and/or creation of interstitial cavities due to incomplete coverage of the filler surface.[43−45] Therefore, it is possible that increased diffusivity in PTMSP/SiO_2 nanocomposites due to presence of interstitial cavities occurs at lower filler contents (≥20 wt %) than what has been observed in the case of filled rubbers.[42]

Conclusions

Interstitial mesopores were observed in PTMSP/fumed silica nanocomposites at filler concentrations between 10 and 50 wt % and in as-received fumed silica. Because of polymer segments partially filling these interstitial cavities in the PTMSP/SiO_2 nanocomposites, the mean radius decreased with decreasing filler concentration. The interstitial mesopore size distribution was sharper in the PTMSP/fumed silica than in the neat fumed silica.

The mean size of the larger free volume cavities in the bimodal free volume size distribution in PTMSP increased significantly with increasing filler concentration. The significant increase even at relatively low filler concentrations (20 wt %) indicated that the filler particles affect the free volume sizes at longer length scales that what is generally observed in polymers. The larger free volume cavity size distribution in PTMSP was broadened with increasing filler concentration, indicating that the filler particles affect only a fraction of the polymer, presumably polymer segments close to the filler surface.

A clear correlation between nitrogen gas permeability and interstitial cavity volume was observed, and the permeability increased with increasing filler content (>10 wt %). The interstitial cavities have a significant positive effect on the permeability of gases in PTMSP/fumed silica nanocomposite membranes, which outweighs the generally observed effect of reduced diffusivity when impenetrable fillers are incorporated into a polymeric membrane.

Acknowledgment. The authors thank John Algers and Morten Eldrup for valuable discussions. The Swedish Research Council is acknowledged for financial support.

References and Notes

(1) Pandey, P.; Chauhan, R. S. *Prog. Polym. Sci.* **2001**, *26*, 853−893.
(2) Stern, S. A. *J. Membr. Sci.* **1994**, *94*, 1−65.
(3) Park, G. S. In *Diffusion in Polymers*; Crank, J., Park, G. S., Eds.; Academic Press: London, 1968; pp 141−163.
(4) Zhang, T.; Litt, M. H.; Rogers, C. E. *J. Polym. Sci., Part B: Polym. Phys.* **1994**, *32*, 1671−1676.
(5) Tanaka, K.; Kita, H.; Masaaki, O.; Okamoto, K. *Polymer* **1992**, *33*, 585−592.
(6) McHattie, J. S.; Koros, W. J.; Paul, D. R. *Polymer* **1991**, *32,* 840−850.
(7) Aitken, C. L.; Koros, W. J.; Paul, D. R. *Macromolecules* **1992**, *25*, 3424−3434.
(8) Yampolskii, Y. P.; Korikov, A. P.; Shantarovich, V. P.; Nagai, K.; Freeman, B. D.; Masuda, T.; Teraguchi, M.; Kwak, G. *Macromolecules* **2001**, *34,* 1788−1796.
(9) Nagel, C.; Gunther-Schade, K.; Fritsch, D.; Strunskus, T.; Faupel, F. *Macromolecules* **2002**, *35*, 2071−2077.
(10) Cohen, M. H.; Turnbull, D. *J. Chem. Phys.* **1959**, *31*, 1164−1169.
(11) Frisch, H. L.; Klempner, D.; Kwei, T. K. *Macromolecules* **1971**, *4*, 237−238.
(12) Fujita, H. *Fortschr. Hochpolym.-Forsch.* **1961**, *3*, 1−47.
(13) Vieth, W. R.; Eilenberg, J. A. *J. Appl. Polym. Sci.* **1972**, *16*, 945−954.
(14) Petropoulos, J. H. *J. Polym. Sci., Part A-2: Polym. Phys.* **1970**, *8*, 1797.
(15) Paul, D. R.; Koros, W. J. *J. Polym. Sci., Part B: Polym. Phys.* **1976**, *14*, 675−685.
(16) Booij, H. C. *Br. Polym. J.* **1977**, *9*, 47−55.
(17) Hong, X.; Jean, Y. C.; Yang, H. J.; Jordan, S. S.; Koros, W. J. *Macromolecules* **1996**, *29*, 7859−7864.
(18) Stannett, V. In *Diffusion in Polymers*; Crank, J., Park, G. S., Eds.; Academic Press: London, 1968; pp 41−73.
(19) Masuda, T.; Isobe, E.; Higashimura, T. *Macromolecules* **1985**, *18*, 841−845.
(20) Takada, K.; Matsuya, H.; Masuda, T.; Higashimura, T. *J. Appl. Polym. Sci.* **1985**, *30*, 1605−1616.
(21) Pinnau, I.; Toy, L. G. *J. Membr. Sci.* **1996**, *116*, 199−209.
(22) Srinivasan, R.; Auvil, S. R.; Burnban, P. M. *J. Membr. Sci.* **1994**, *86*, 67−86.
(23) Wästlund, C.; Maurer, F. H. J. *Polymer* **1998**, *39*, 2897−2902.
(24) Kim, I. W.; Lee, K. J.; Jho, J. Y.; Park, H. C.; Won, J.; Kang, Y. S.; Guiver, M. D.; Robertson, G. P.; Dai, Y. *Macromolecules* **2001**, *34*, 2908−2913.
(25) Zax, D. B.; Yang, D. K.; Santos, R. A.; Hegemann, H.; Giannelis, E. P.; Manias, E. *J. Chem. Phys.* **2000**, *112*, 2945−2951.
(26) Litvinov, V. M.; Spiess, H. W. *Macromol. Chem.* **1991**, *192*, 3005−3019.
(27) Kwiatkowski, J.; Whittaker, A. K. *J. Polym. Sci., Part B: Polym. Phys.* **2001**, *39*, 1678−1685.
(28) Kirst, K. U.; Kremer, F.; Litvinov, V. M. *Macromolecules* **1993**, *26*, 975−980.
(29) Anastasiadis, S. H.; Karatasos, K.; Vlachos, G.; Manias. E.; Giannelis, E. P. *Phys. Rev. Lett.* **2000**, *84*, 915−918.
(30) Krishnamoorti, R.; Vaia, R. A.; Giannelis, E. P. *Chem. Mater.* **1996**, *8*, 1728−1734.
(31) Vaia, R. A.; Sauer, B. B.; Tse, O. K.; Giannelis, E. P. *J. Polym. Sci., Part B: Polym. Phys.* **1997**, *35*, 59−67.
(32) Yim, A.; St. Pierre, L. E. *Polym. Lett.* **1969**, *7*, 237−239.
(33) Winberg, P.; Eldrup, M.; Maurer, F. H. J. *Polymer* **2004**, *45*, 8253−8264.
(34) Algers, J.; Suzuki, R.; Ohdaira, T.; Maurer, F. H. J. *Macromolecules* **2004**, *37*, 4201−4210.
(35) He, C.; Hamada, E.; Suzuki, T.; Kobayashi, H.; Kondo, K.; Shantarovich, V. P.; Ito, Y. *J. Radioanal. Nucl. Chem.* **2003**, *255*, 431−435.
(36) Algers, J.; Suzuki, R.; Ohdaira, T.; Maurer, F. H. J. *Polymer* **2004**, *45*, 4533−4539.
(37) Jean, Y. C.; Cao, H.; Dai, G. H.; Suzuki, R.; Ohdaira, T.; Kobayashi, Y.; Hirata, K. *Appl. Surf. Sci.* **1997**, *116*, 251−255.
(38) Merkel, T. C.; Freeman, B. D.; Spontak, R. J.; He, Z.; Pinnau, I.; Meakin, P.; Hill, A. J. *Science* **2002**, *296*, 519−522.
(39) Merkel, T. C.; Freeman, B. D.; Spontak, R. J.; He, Z.; Pinnau, I.; Meakin, P.; Hill, A. J. *Chem. Mat.* **2003**, *15*, 109−123.
(40) Merkel, T. C.; He, Z. J.; Pinnau, I.; Freeman, B. D.; Meakin, P.; Hill, A. J. *Macromolecules* **2003**, *36*, 8406−8414.
(41) Merkel, T. C.; He, Z. J.; Pinnau, I.; Freeman, B. D.; Meakin, P.; Hill, A. J. *Macromolecules* **2003**, *36*, 6844−6855.
(42) Barrer, R. M. In *Diffusion in Polymers*; Crank, J., Park, G. S., Eds.; Academic Press: London, 1968; pp 165−217.
(43) Duval, J. M.; Kemperman, A. J. B.; Folkers, B.; Mulder, M. H. V.; Desgrandchamps, G.; Smolders, C. A. *J. Appl. Polym. Sci.* **1994**, *54*, 409−418.
(44) Mahajan, R.; Koros, W. J. *Polym. Eng. Sci.* **2002**, *42*, 1420−1431.
(45) Zimmerman, C. M.; Singh, A.; Koros, W. J. *J. Membr. Sci.* **1997**, *137*, 145−154.
(46) Mogensen, O. In *Positron Annihilation in Chemistry*; Goldanskii, V. I., Schäfer, F. P., Toennies, J. P., Eds.; Springer-Verlag: Berlin, 1995; pp 48−65.
(47) Eldrup, M.; Lightbody, D.; Sherwood, J. N. *Chem. Phys.* **1981**, *63*, 51−58.
(48) Nakanishi, H.; Yean, Y. C. In *Positron and Positronium Chemistry*; Schrader, D. M., Jean, Y. C., Eds.; Elsevier: Amsterdam, 1988; pp 159−192.
(49) Tao, S. J. *J. Chem. Phys.* **1972**, *56*, 5499.
(50) Kirkegaard, P.; Pedersen, N.; Eldrup, M. Risø-M-2740, Risoe National Laboratory, 1989.
(51) Shukla, A.; Peter, M.; Hoffmann, L. *Nucl. Instrum. Methods A* **1993**, *335*, 310−317.
(52) Mogensen, O. In *Positron Annihilation in Chemistry*; Goldanskii, V. I., Schäfer, F. P., Toennies, J. P., Eds.; Springer-Verlag: Berlin, 1995; pp 66−87.
(53) Iler, R. K. In *Chemistry of Silica*; John Wiley and Sons: New York, 1979.
(54) Zaleski, R. In *Positronium Lifetime Tables*, Institute of Physics, Marie Curie-Sklodowska University; EL-Press: Lublin, 2002.
(55) Goworek, T.; Ciesielski, K.; Jasinksa, B.; Wawryszczuk, J. *Chem. Phys.* **1998**, *230*, 305−315.
(56) Bi, J. J.; Wang, C. L.; Kobayashi, Y.; Ogasawara, K.; Yamasaki, A. *J. Appl. Polym. Sci.* **2003**, *87*, 497−501.
(57) Consolati, G.; Genco, I.; Pegoraro, M.; Zanderighi, L. *J. Polym. Sci., Part B: Polym. Phys.* **1996**, *34*, 357−367.
(58) Wang, X. Y.; Lee, K. M.; Lu, Y.; Stone, M. T.; Sanchez, I. C.; Freeman, B. D. *Polymer* **2004**, *45*, 3907−3912.
(59) Arrighi, V.; Higgins, J. S.; Burgess, A. H.; Floudas, G. *Polymer* **1998**, *39*, 6369−6376.
(60) Maurer, F. H. J.; Welander, M. *J. Adhes. Sci. Technol.* **1991**, *5*, 425−437.
(61) Hamielec, A. E.; Eldrup, M.; Mogensen, O.; Jansen, P. *J. Macromol. Sci., Rev. Macromol. Chem. Phys.* **1973**, *C9*, 305−337.
(62) DeSitter, K.; et al. To be submitted for publication.

MA047369J